Climate Dynamics (2021) 56:651–664
https://doi.org/10.1007/s00382-020-05496-9

On the connection between AMOC and observed land precipitation in Northern Hemisphere: a comparison of the AMOC indicators

Jing Zhang[1] · Yusen Liu[1] · Cheng Sun[1] · Jianping Li[2,3] · Ruiqiang Ding[4] · Fei Xie[1] · Tiejun Xie[1] · Yazhou Zhang[2] · Zhanqiu Gong[1]

Received: 15 May 2020 / Accepted: 9 October 2020 / Published online: 26 October 2020

Abstract

Decadal climate prediction has been one of the most popular topics in recent climate change studies. It is closely linked to our daily life, deeply affecting the wellbeing of people and global economic growth. Among those climate variables, precipitation is essential for industrial and agricultural productions but it's also hard to precisely predict. In this study, we provide observational evidence for the relationship of mean precipitation in the Northern Hemisphere (NH), NH tropics and Sahel with the five Atlantic Meridional Overturning Circulation (AMOC) indicators on the multidecadal time scale. We conclude that precipitation in those three regions exhibits a consistent multidecadal variability from 1901 to 2015. The correlations between NH precipitation and AMOC indicators are strong and significant. The NAO-based AMOC indicator leads the precipitation by 8 years and the correlation coefficient reaches 0.9 higher than other oceanic indicators. It is the NAO that forces the AMOC transporting heat to the North Atlantic and induces sea surface temperature (SST) dipole which eventually affects the multidecadal precipitation change in NH. As the AMOC_NAO indicator leads the precipitation, we employ it as a predictor and construct a linear model to make a future prediction based on historical data. It indicates that the precipitation will decrease in the following few years, and then will rise again.

Keywords AMOC indicator · Northern Hemisphere precipitation · Multidecadal variability

1 Introduction

The Northern Hemisphere (NH) has the largest land and sea, and about 90% of the world's population lives in the NH. Complex geological relationships make it even harder to fully understand the NH climate system under the circumstances of anthropogenic climate change. Thus, it's worth investigating the natural variability in NH and managing to make future predictions. Multidecadal climate prediction is essential in contemporary climatological studies (Boer 2011; Meehl et al. 2009) and has been listed as a core of Coupled Model Inter-comparison Project (CMIP). Decadal Climate Prediction Project (DCPP) has been initiated to work on such topics (Boer et al. 2016). Many studies have focused on the predicting skill of sea surface temperature (SST) and surface air temperature (Li et al. 2013; Xie et al. 2019), but decadal changes in precipitation still require further investigations. Unlike the relatively skillful prediction in temperature, uncertainty in data and complex mechanisms limit our ability to make a precise prediction in precipitation on

Electronic supplementary material The online version of this article (https://doi.org/10.1007/s00382-020-05496-9) contains supplementary material, which is available to authorized users.

✉ Cheng Sun
scheng@bnu.edu.cn

[1] College of Global Change and Earth System Science (GCESS), Beijing Normal University, Beijing 100875, China

[2] Frontiers Science Center for Deep Ocean Multispheres and Earth System (FDOMES)/Key Laboratory of Physical Oceanography/Institute for Advanced Ocean Studies, Ocean University of China, Qingdao 266100, China

[3] Laboratory for Ocean Dynamics and Climate, Pilot Qingdao National Laboratory for Marine Science and Technology (QNLM), Qingdao 266237, China

[4] State Key Laboratory of Earth Surface Processes and Resource Ecology, Beijing Normal University, Beijing 100875, China

the multidecadal time scale and the predicting performance remains low over the globe (Doblasreyes et al. 2013).

Previous studies have pointed out that the decadal variation in precipitation is related to ocean thermal and dynamical processes. For example, the SST warming associated with the Atlantic Multidecadal Oscillation (AMO) changes the precipitation over regional (Sun et al. 2015a, c; Teegavarapu et al. 2013; Veres and Hu 2013) and continental scale (Garciagarcia and Ummenhofer 2015). Besides, the El Niño-Southern Oscillation (ENSO) (Barlow et al. 2001; Hu and Feng 2012), Indian Ocean Dipole (IOD) and Pacific Decadal Oscillation (PDO) (Valdespineda et al. 2018) are also related to the decadal precipitation variations.

Above all, the Atlantic Meridional Overturning Circulation (AMOC) is one of the most important ocean dynamics in the world and it profoundly influences the multidecadal climate changes in Atlantic and the adjacent areas through the anomalous ocean heat transport from one hemisphere to the other (Buckley and Marshall 2016; Delworth and Mann 2000; Lee and Wang 2010; Trenberth and Caron 2001). AMOC is forced by the persistent wind anomalies related to the NAO and exhibits delayed responses to the atmosphere by 15 years (Sun et al. 2015b). AMOC plays an intermedia role by storing the anomalous atmospheric signals into the ocean, further inducing changes in Atlantic SST which could influence the climate in distance through the atmospheric teleconnections (Fred et al. 2016; Li et al. 2016). It is also suggested that the AMOC can restore the anthropogenic heat and buffer global warming (Chen and Tung 2018). In recent years, scientists have found the close relationships between AMOC and precipitation over the remote regions like America (Burckel et al. 2015; Parsons et al. 2014) and East Asia based on model simulations. Besides, variations in the AMOC are also connected to the precipitation in Sahel (Wang et al. 2012) and influence the monsoon over Africa (Vellinga and Wood 2002).

However, model simulation alone is not enough to fully determine the relationship between AMOC and NH precipitation. Biases largely originate from model uncertainties and the simulation results are varied among models. Observational evidence is needed to confirm the findings in previous studies and further explain the mechanism. Since the NAO leads AMOC by about 15 years, it is also important to highlight the role of NAO-related indices in predicting the precipitation associated with the AMOC. In this study, we find the multidecadal variability in precipitation over NH, NH tropics (0°–20°N) and Sahel (10°–20°N, 20°W–30°E) from 1901 to 2015. We also re-examined correlations between precipitation and AMOC indicators based on the observed oceanic and atmospheric variables and evaluate their influences. Using observational data, we attempt to explain how the AMOC influences the precipitation through the SST Dipole. Eventually, we construct a linear model to predict future changes in NH precipitation using AMOC_NAO as a predictor.

This paper is organized as follows: Sect. 2 is the data and detailed information about AMOC indicators. Results are given in Sect. 3. Our conclusion and discussion can be seen in the final section.

2 Data and methods

In this study, we employ five indices as the AMOC indicators. They are mainly distinguished by their definitions, data sources and time lengths. We retrospect these indicators and make further inter-comparisons in this section.

2.1 AMOC_SST index

Rahmstorf et al. (2015) defined it by subtracting the Northern Hemisphere mean SST from the mean SST in NH subpolar gyre where it is deemed to be one of the most sensitive regions with respect to the AMOC. Thus, it can represent the long-term variations in AMOC. Based on that, Caesar et al. (2018) redefined a similar index, using the NH subpolar gyre mean SST from November to the 5th month of the following year minus the global mean SST in the same period. It covers the period from 1871 to 2018:

$$AMOC\_SST = \overline{SST_{sg}} - \overline{SST_{global}}.$$

It is noted by Caesar et al. that a long-term linear trend should be removed to better represent the multidecadal variation in AMOC (Caesar et al. 2018). The AMOC_SST index is detrended and normalized to make comparisons with other AMOC indicators.

2.2 AMOC_SUBT$_{400}$ index

This index is calculated by the leading mode of the detrended subsurface sea temperature anomalies observed in the subtropical North Atlantic with a depth of 400 m, covering the period from 1955 to 2015 (Yan et al. 2017; Zhang 2008). Zhang et al. (2008) believe that the subsurface temperature is connected to the ocean circulation in the North Atlantic and it can reveal the changes in the subpolar gyre associated with the ocean dynamics. In consequence, it is capable of representing the variation in AMOC.

2.3 AMOC_SAL$_I$ and AMOC_SAL$_E$ indices

It is also suggested that the subpolar ocean salinity could indicate the AMOC variability. Chen and Tung (2018) defined the index by integrating the ocean salinity from 1500 m depth to the surface and the integral is restricted

in North Atlantic between 45°N and 65°N. The difference between these two salinity-based indices is the data sources. The AMOC_SAL$_I$ is derived from ISHII and Scripps datasets from 1946 to 2015, while the AMOC_SAL$_E$ is obtained from the EN4 dataset from 1946 to 2016. These datasets hold a temporal resolution of the month. Thus, annual mean is then applied onto the original data to unify the timescale with other indicators.

2.4 AMOC_NAO index

Previous modeling studies suggested the NAO plays a key role in modulating AMOC multidecadal variability (Oreilly et al. 2016; Sun et al. 2015b). Persistent forcing is imposed onto the North Atlantic Ocean through the NAO-induced wind anomalies. Owing to the ocean inertia, it changes the ocean circulation with a time lag of approximately 15 years (Gulev and Latif 2015; Sun et al. 2015b). Based on that, this index is defined by the time integration of the NAO index. It characterizes the accumulated forcing of NAO that is imposed onto the ocean circulation thus is capable of reconstructing the AMOC multidecadal variation (Mccarthy et al. 2015; Mecking et al. 2014; Sun et al. 2020):

$$\int_{t_0}^{t} NAO(t)dt$$

where t_0 and t represent the initial year and the final year of the integration, respectively.

The above indicators characterize the variation in AMOC using a variety of variables and can be distinguished by their physical connections with the AMOC. The AMOC_NAO index is the only one that corresponds to the atmospheric circulation, as it is the accumulated forcing of the NAO. The other four indices are related to the surface and subsurface oceanic variables, such as ocean temperature and salinity.

In this study, SST data from 1891 to 2019 uses the COBE dataset (https://www.esrl.noaa.gov/psd/data/gridded/data.cobe.html), with a spatial resolution of $1° \times 1°$. The precipitation data is obtained from CRU (version 4.02), covering the period from 1901 to 2017. NAO index (Hurrell 1995) is also employed from 1899 to 2018. The interdecadal Pacific oscillation (IPO) index from 1955 to 2015 is based on the ERSST v5 dataset (https://psl.noaa.gov/data/timeseries/IPOTPI/). We also employ precipitation data from the Global Precipitation Climatology Centre (GPCC) (Becker et al. 2013) and SST data from the HadISST (Rayner 2003) and NOAA ERSST to validate our results. Moreover, we use the RAPID AMOC at 26.5°N (http://www.rapid.ac.uk/rapidmoc/rapid_data/).

Two-tailed student's *t* test is used here to access the statistical significance of two auto-correlated variables in the low-pass filtered time series using the effective number of degrees of freedom. It has been broadly used in previous studies which were mainly focusing on the multidecadal climate variability (Li et al. 2013; Sun et al. 2015c, 2017). The effective number of degrees of freedom is given by (Pyper and Peterman 1998):

$$\frac{1}{N^{eff}} \approx \frac{1}{N} + \frac{2}{N}\sum_{j=1}^{N}\frac{N-j}{N}\rho_{XX}(j)\rho_{YY}(j), \quad (1)$$

where N represents the sample size and $\rho_{XX}(j)$ and $\rho_{YY}(j)$ are the autocorrelations of two sampled time series X and Y at a lag time j. It has been suggested that the N^{eff} of order 2 determined by Eq. (1) is rigorous and appropriate for the significance tests of correlation (Bretherton et al. 1999). In this study, to test the significance for a correlation map we first calculate the corresponding N^{eff} for each individual grid cell (based on the time series at each grid cell) using Eq. (1) and then estimate the correlation thresholds required to meet the significance level (as shown in Fig. S1 in Supplementary Materials).

3 Result

3.1 Characteristics of NH multidecadal variability in precipitation

Figure 1 shows the time series of normalized AMOC indicators (1955–2015) and measured RAPID at 26°N (2004–2015). These indicators generally display AMOC characteristics of consistent multidecadal variation for this period, with the AMOC_NAO leading by about 5 years compared to the other four oceanographic reconstructions. The AMOC strength is relatively strong before the 1960s and shows a trend of fluctuating decrease during 1975–1995. Until the beginning of the twenty-first century it gradually increased. Then the reconstructed AMOC indicators all show a weakening trend since 2005, similar to the change of the measured RAPID (available from 2004).

Previous studies suggested that decadal variation in NH precipitation is related to ocean thermal and dynamical processes. Then time series of the annual mean precipitation in NH, NH tropics and Sahel from 1901 to 2015 are first examined. Despite the discrepancy in quantity, precipitation in all three regions shares a similar variability as shown in Fig. 2. Moreover, in Fig. 2b, the 11-year running mean precipitation series exhibits significant multidecadal variability, although the amplitude is relatively low before 1920, varying within 2 mm/month. A sudden rise of the mean precipitation first appears in the Sahel around 1920 and later in NH tropics. The mean precipitation in both Sahel and NH tropics meet their first maxima in 1930 while the mean precipitation over the entire NH remains unchanged until 1940. The changes

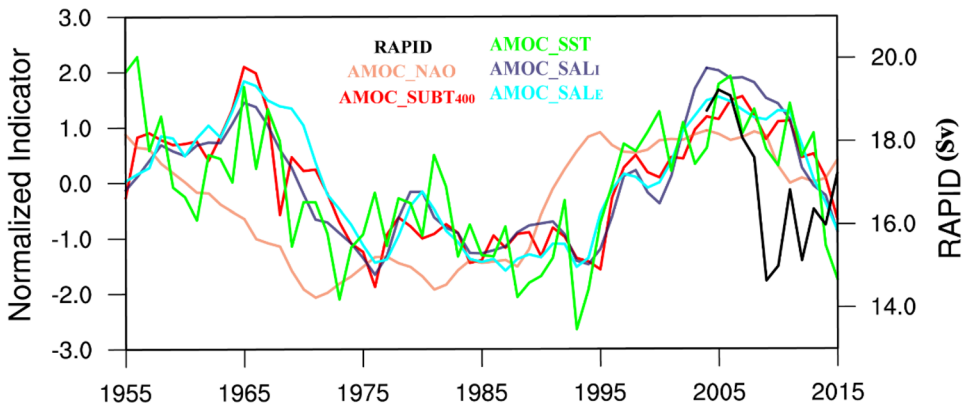

Fig. 1 Time series of the normalized AMOC indicators (1955–2015) and measured RAPID (2004–2015). The measured RAPID (black) is calculated by the maximum of the transport streamfunction. See Sect. 2 for AMOC indicator details

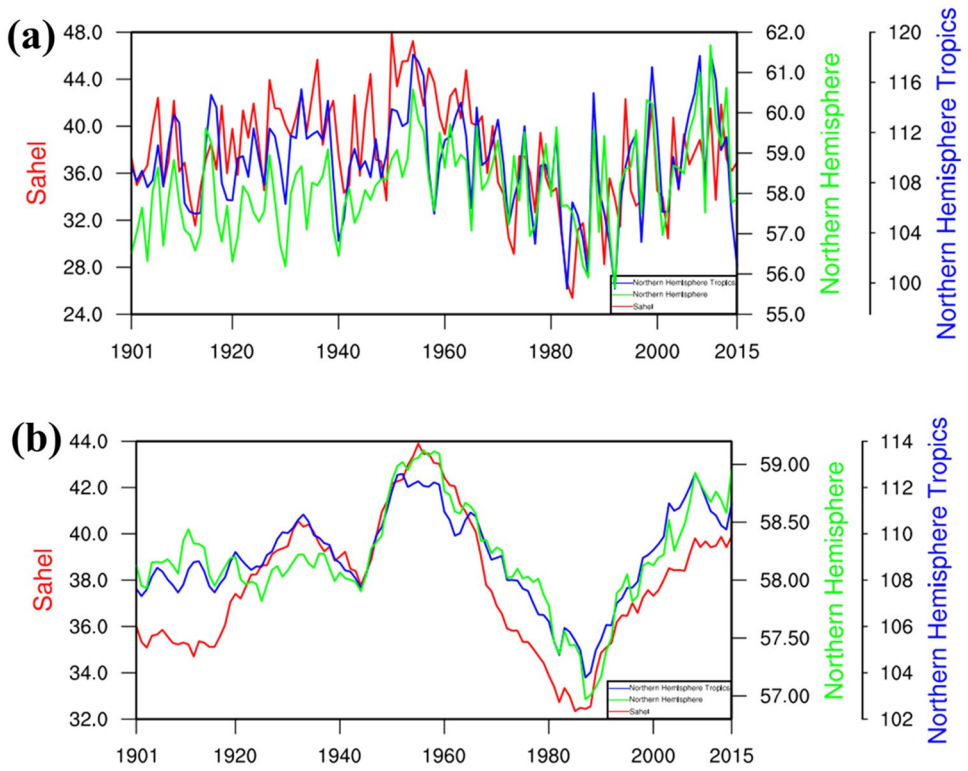

Fig. 2 **a** Time series of precipitation (mm/month) in the Sahel (red line), Northern Hemisphere (green line) and Northern Hemisphere Tropics (blue line) for the period 1901–2015. **b** As in **a**, but for the detrended 11-year running mean precipitation data

in extra-tropics may compensate for the slight fluctuations in Sahel and NH tropics and it could explain the mild feedback over the entire NH. Since 1940, the amplitudes in precipitation variations among three regions become higher and the most pronounced change occurs in the Sahel, with the amplitude varies between 32 and 44 mm/month from 1940 to 2015. The amplitude in the entire NH is relatively low but still significant, considering its large spatial scale. More importantly, trends in mean precipitation variations over Sahel, NH tropics and NH are highly consistent. Increasing trends in mean precipitation could be detected from all three regions in the late 1940s and 1950s and then reach maxima around 1955. In the following three decades, the mean precipitation in Sahel, NH tropics and NH experiences significant decreasing trends. After reaching the minimum values at 32, 104 and 57 mm/month in the Sahel, NH tropics and NH, respectively, mean precipitation starts to increase once again in 1988. It is apparent that the multidecadal variability in NH mean precipitation does exist and it is more pronounced in Sahel and NH tropics based on the observational data from 1901 to 2015, but it should be noted that the variability is more significant after 1940, which needs further investigation.

3.2 Association of NH precipitation and AMOC indictors

Previous modeling studies have suggested close connections between multidecadal variations in precipitation and

ocean dynamics (Sun et al. 2013). The AMOC has long been recognized as an important part of the global ocean circulation and its strength profoundly affects temperature and precipitation over the adjacent continents and even the entire Northern Hemisphere (Srokosz et al. 2012). Thus, we try to find out the connections between the AMOC and NH mean precipitation using some AMOC indictors. Since these AMOC indicators and precipitation are based on observation instead of model simulation, it provides more observational evidence for the close relationship of the AMOC with NH precipitation. Simultaneous correlations between detrended 11-year running mean NH precipitation data and five AMOC indicators from 1955 to 2015 are shown in Fig. 3. All five indicators exhibit consistent spatial patterns associated with the NH mean precipitation. Strong and significant positive correlations can be found over the Sahel and northeastern Siberia while the negative correlations occur in North America, Arabian Peninsula and Iranian Plateau, but it's relatively weak. It should be noted that the correlations between AMOC indicators and mean precipitation in the Sahel are more significant than other regions with a correlation coefficient larger than 0.6, except for AMOC_SST indictor. Thus, we can conclude that the observed precipitation in the Sahel shows clear simultaneous correlations with the AMOC indicators using subsurface and atmospheric variables and its relationship with the subsurface sea temperature is more prominent than other indicators, as the correlation is statistically significant over the most area in the Sahel and the coefficient is larger than 0.8. Since the AMOC_SST is defined by the SST in a limited area (NH subpolar gyre), the relationship between North Atlantic and Sahel precipitation may not be completely captured by the SST indicator, further explaining why the correlation is relatively low. Also, the precipitation data without preprocessing also exhibits qualitatively similar results, as shown in Fig. S2.

However, simultaneous correlations may not be enough to fully reveal the relationship between the mean precipitation in Northern Hemisphere and AMOC indicators. Those indicators are constructed using oceanographic and atmospheric variables, which may not simultaneously represent the strength of AMOC. For instance, the AMOC_NAO index is defined by the accumulated atmospheric forcing and it would lead the AMOC by several years. Then, we carried out lead-lag correlations (Fig. 4) among AMOC indicators and the mean precipitation in NH, NH tropics and Sahel, respectively. In Fig. 4a, the AMOC_NAO index exhibits the most prominent correlation with the NH precipitation when it leads by 8–9 years. The correlation coefficient reaches 0.9, higher than other indicators at the same time lag. However, for those indicators with oceanographic variables, the maximum correlation coefficients with NH precipitation are below 0.8 at a time lag within 5 years. We further investigate

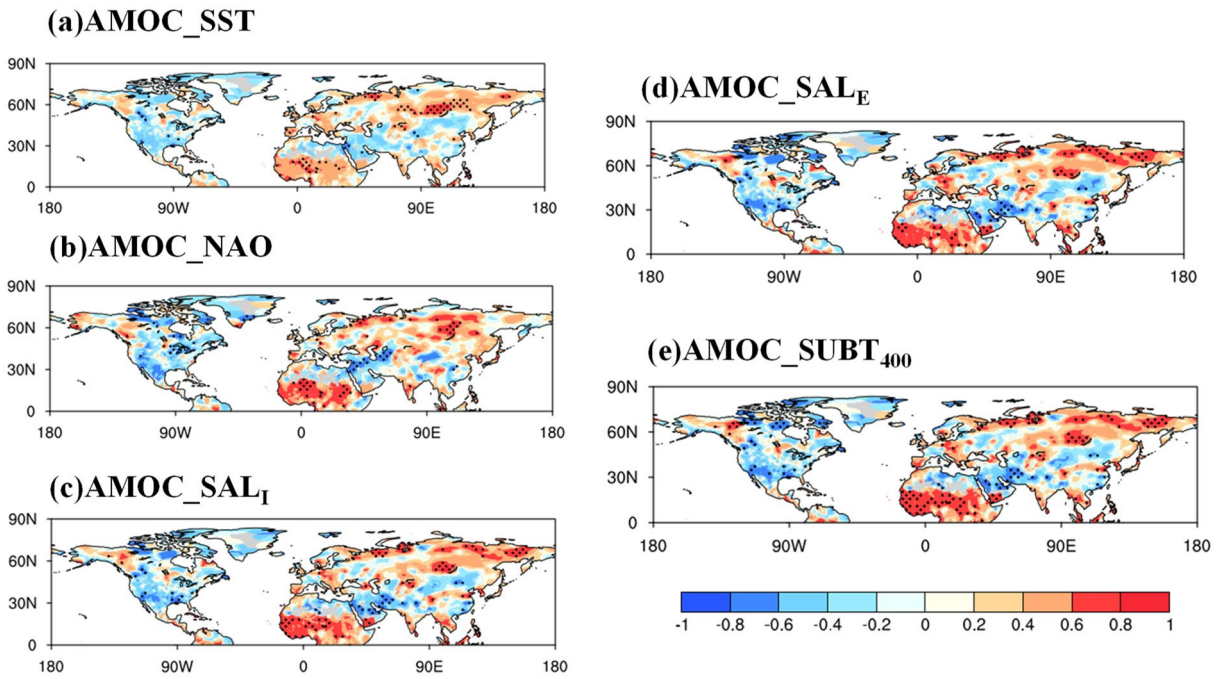

Fig. 3 Simultaneous correlations between AMOC indicators and the observed Northern Hemisphere annual mean precipitation based on the CRU dataset for the period 1955–2015. The precipitation data was processed by the 11-year running mean and the long-term linear trend was removed to isolate the decadal-scale variability by removing the least-squares linear trend of the data from all grid points. The dotted areas denote correlations significantly above the 95% confidence level using the effective number of degrees of freedom

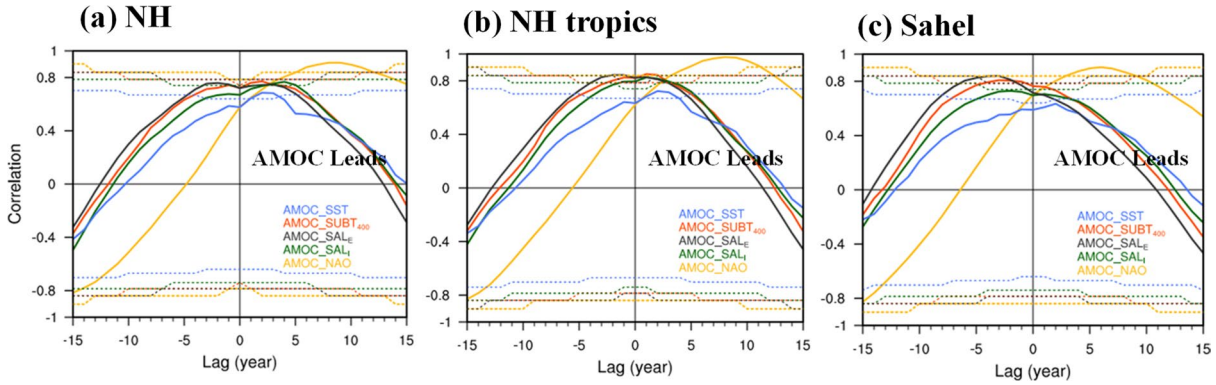

Fig. 4 Lead-lag correlations between normalized AMOC indicators and the detrended 11-year running mean precipitation in Northern Hemisphere (**a**), Northern Hemisphere tropics (**b**) and Sahel (**c**) during the period 1955–2015. The dotted lines denote the 95% confidence levels for the correlations using the effective number of degrees of freedom

the correlations between AMOC and mean precipitation in NH tropics and Sahel, shown in Fig. 4b, c. The AMOC_NAO index also exhibits the most prominent correlation with the mean precipitation over these areas, consistent with the findings in NH. It needs to point out that the correlation coefficient is close to 1 when the AMOC_NAO index leads the mean precipitation in NH tropics by nearly 8 years. Besides, the oceanic indicators using sea salinity and subsurface temperature are correlated with the mean precipitation in NH tropics simultaneously, since the coefficients reach their maxima (0.8) without any delay. However, in the Sahel, those indicators significantly correlate with mean precipitation at a time lag of 5 years. In other words, the response of precipitation in the Sahel to the AMOC, for some reason, is delayed than those in NH tropics and the entire Northern Hemisphere. Correlation coefficients of the AMOC_SST index are the lowest, comparing to other indicators in all three regions. However, unlike those indices using salinity or oceanographic subsurface variables, the AMOC_SST reaches its maximum when it leads the mean precipitation by 2–3 years. In order to validate our results, we repeat our analysis by using the GPCC data (Fig. S7) and the results are fairly close to the CRU data. Also, the raw data exhibits similar results, as is shown in Fig. S3. In conclusion, lead-lag correlations suggest that all five AMOC indicators have positive correlations with the mean precipitation in NH, NH tropics and Sahel. Such a result is consistent with that in the simultaneous correlation, indicating the connection between AMOC and the mean precipitation in NH is strong and robust with and without any time lag. More importantly, the AMOC_NAO index exhibits the most prominent correlation (larger than 0.8) with the mean precipitation in NH, NH tropics and Sahel when it leads by 8 years, whereas correlation coefficients of other indices using oceanographic variables reach their maxima without any time lag and the maximum values are smaller than that with AMOC_NAO index in all three regions. It indicates that the AMOC_NAO index is not only capable of explaining the multidecadal variability in NH mean precipitation, but also has the unique potentials to predict the mean precipitation in NH by around 8 years while oceanographic indicators are basically in phase with it. Since the AMOC_NAO index is defined by the accumulated forcing of the NAO, which leads the AMOC by 15 years due to the large ocean inertia in association with the slow oceanic processes, it could be an extension for our understanding about the predictability in multidecadal variations of the NH mean precipitation.

In Fig. 5, the spatial patterns of the lead-lag correlations between AMOC indicators and the detrended 11-year running mean precipitation in NH are also examined. When the indicators lead by 8 years, the correlation patterns are consistent with those in Fig. 3, but the strength of the correlations are varied among indicators. It is clearly shown that, in this case, the correlation between AMOC_NAO index and NH mean precipitation is more prominent than other indicators and it's even more significant than the simultaneous correlation. It further supports our previous findings that the AMOC_NAO index strongly connects to the NH precipitation and it leads the precipitation by 8 years. Although the correlations between NH mean precipitation and AMOC indicators are overall positive as suggested in Fig. 4, the spatial distribution of the responses is quite different as positive correlations can be found over northeastern Siberia and Sahel while the negative correlations located over North America, western Siberia and Arabian Peninsula. Moreover, comparing with the spatial patterns without any time lag (Fig. 3), it highlights the leading role of the AMOC_NAO index and indicates the different responses of regional precipitation to those oceanic indicators as well. The correlations in the Sahel and northeastern Siberia (Fig. 5) are significantly strengthened with the AMOC_NAO index at a time lag of 8 years while other indices exhibit weakened

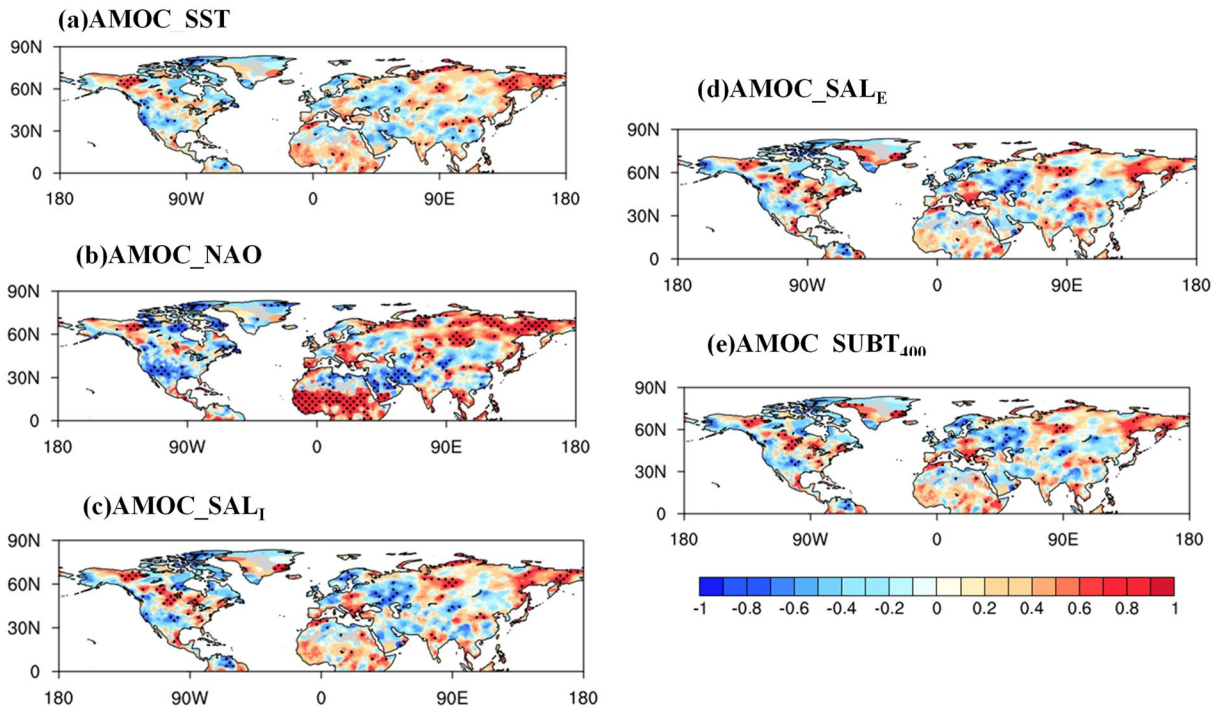

Fig. 5 Lead-lag correlations of AMOC indicators with the annual mean precipitation in the Northern Hemisphere for the period 1955–2015. All five indices lead the precipitation by 8 years. The precipitation data were detrended and processed with an 11-year running mean. The dotted areas denote correlations significantly above the 95% confidence level using the effective number of degrees of freedom

correlations, especially in the Sahel region. It is also suggested that the AMOC_NAO indicator strongly correlates with the NH precipitation for the GPCC data (Fig. S6) when it leads by 8 years, further validating our results. Also, the simultaneous correlation patterns for the oceanic indicators using GPCC data (Fig. S6) are consistent with those using CRU data.

In this study, we use five AMOC indicators to represent the strength of the AMOC. We find that the connection between the AMOC strength and the precipitation is different among the indicators. Therefore, it is of great importance to quantitatively analyze their connections to the NH, NH tropics and Sahel precipitation for individual AMOC indicators. Based on the lead-lag correlations (Fig. 4), we have found the oceanic indices of the AMOC are simultaneously correlated with the precipitation in NH, NH tropics and Sahel, while the NAO-based index shows the most prominent correlation when it leads the precipitation by 8 years. Then, we evaluated the AMOC impact by regressing the annual mean precipitation over different regions onto each indicator, and for the AMOC_NAO, the index leads the precipitation by 8 years. As shown in Fig. 6, the AMOC_NAO index has the best performance in explaining the multidecadal variability of the annual mean precipitation in all three regions. It indicates that the correlation between AMOC and NH precipitation can be better depicted using the AMOC_NAO index. Additionally, the indices using subsurface ocean salinity and temperature also relate to the precipitation in those regions but they are not as good as the AMOC_NAO index. We may infer that the ocean dynamics alone is not enough to explain the connections between AMOC and NH precipitation, and this is why the AMOC_NAO index, the only one that combines the effects of the NAO, has the best performance. It indicates that the atmospheric forcing contained in the AMOC indicator is a critical factor that is absent in other indices and it limits our ability in explaining the precipitation in NH only using oceanographic processes. It may lead us to investigate the relationship between the North Atlantic and precipitation in NH from the perspective of air-sea coupling. The poor performance of the AMOC_SST index also supports our idea and emphasizes the importance of deep ocean circulation and the associated interhemispheric salinity transportation. In Fig. 6b, c, the AMOC significantly relates to the precipitation in NH tropics, Sahel and the entire NH and it is consistent among indicators. In conclusion, the AMOC_NAO index is the optimal indicator when we attempt to explain the multidecadal variability in NH mean precipitation using the AMOC signal, mainly because it is highly correlated with the precipitation when it leads by 8 years.

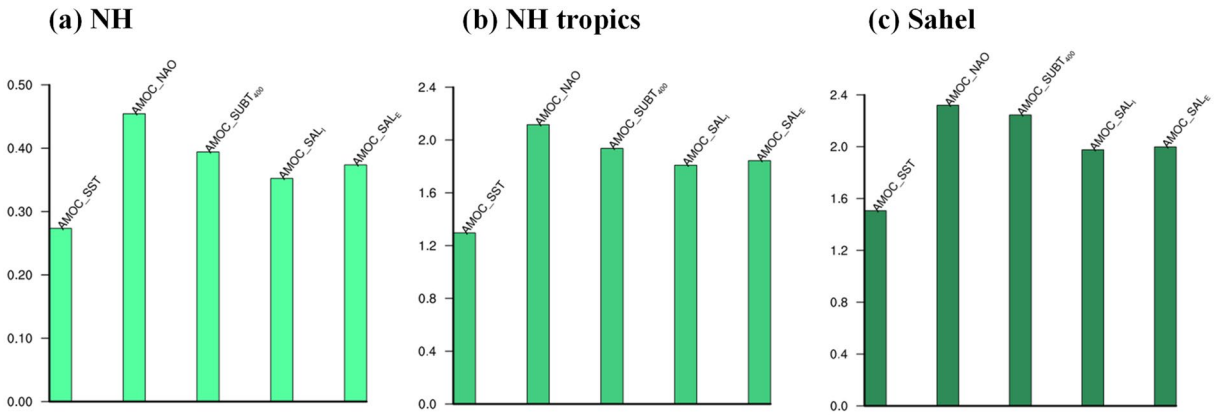

Fig. 6 Regressions of the annual mean precipitation anomalies (mm/month) in Northern Hemisphere (**a**), Northern Hemisphere tropics (**b**) and Sahel (**c**) onto the AMOC indicators. Only the AMOC_NAO index leads the precipitation by 8 years. Precipitation data were detrended and processed with an 11-year running mean

In addition, we calculate the explained variance of decadal precipitation in the NH at each grid cell by the AMOC_NAO indicator when it leads by 8 years (Fig. S4). As shown in Figs. 3 and 5, the AMOC has a close relationship with the decadal precipitation over the NH, especially in the Sahel, eastern Siberia and central North America. The correlation coefficients of decadal precipitations in these regions with the AMOC_NAO indicator reach 0.88, 0.91 and −0.92, respectively. In particular, the AMOC-induced changes can explain 77, 82 and 85% of the rainfall variance in the Sahel, eastern Siberia and central North America (Table S1), respectively. Meanwhile, the previous study (Dong and Dai 2015) has suggested that the IPO (Fig. S5a) can affect regional precipitation. As shown in Fig. S5b, in the Northern Hemisphere, the IPO shows the strongest positive correlation with the decadal precipitation variations over the southwest U.S. To compare the roles of AMOC and IPO in the regional precipitation variability, we list the correlations of decadal precipitation over the Sahel, eastern Siberia and central North America with the AMOC and IPO indices in Table. S1. The corresponding explained variances by the IPO are 15, 19 and 63%, respectively. It indicates that, in these regions, the AMOC plays a more important role in the decadal precipitation variability than the IPO, especially for the Sahel and eastern Siberia.

3.3 Physical mechanism of how the AMOC affects NH precipitation

We have revealed the close relationships between NH mean precipitation and five AMOC indicators and the AMOC_NAO index leads the precipitation by 8 years. In this section, the physical mechanism involved is discussed as follows. Previous modeling studies have suggested that the positive NAO would intensify the AMOC, imposing persistent forcing by the anomalous winds. The strengthened AMOC prompts the northward ocean heat transport from one hemisphere to the other. AMOC-induced ocean heat convergence further leads to SST warming over the upper-level North Atlantic, which is referred to as the AMO. Meanwhile, the opposite sign can be detected over the South Atlantic where there's SST cooling (Keenlyside et al. 2008). The SST pattern induced by the contrasting impacts of AMOC on the North and South Atlantic temperature is referred to as Bipolar Seesaw or Interhemispheric SST Dipole (Broecker 1998; Latif et al. 2004; Sun et al. 2015a, 2018). Here, we define the dipole index by simply subtracting the South Atlantic annual mean temperature from the North Atlantic annual mean temperature. It must note that the Interhemispheric SST Dipole associated with AMO cannot be reproduced only if the ocean circulation is involved in the model simulation (Sun et al. 2018), further emphasizing the intermediary role of AMOC in modulating the SST patterns in the two hemispheres under the persistent atmospheric forcing of NAO. Overall, the sequence is as follows: NAO-AMOC-SST Dipole. Then, we calculate the lead-lag correlations between SST Dipole and five AMOC indicators (Fig. 7). In order to highlight the multidecadal characteristics, the dipole index used in Fig. 7b is detrended and derived from 11-year running mean precipitation data. As shown in Fig. 7b, all AMOC indices have positive correlations with the SST Dipole. Furthermore, the AMOC_NAO index is highly correlated with the SST Dipole when it leads by 6 years and the correlation coefficient passes 0.8 which is higher than other indices. In addition, the AMOC_NAO index is the only one that leads the SST Dipole, whereas other indices using oceanographic variables are lagged by 5 years, except for the AMOC_SST index which is basically synchronized with the SST Dipole. Based on statistical analysis, we can conclude that the AMOC is strongly connected to the SST

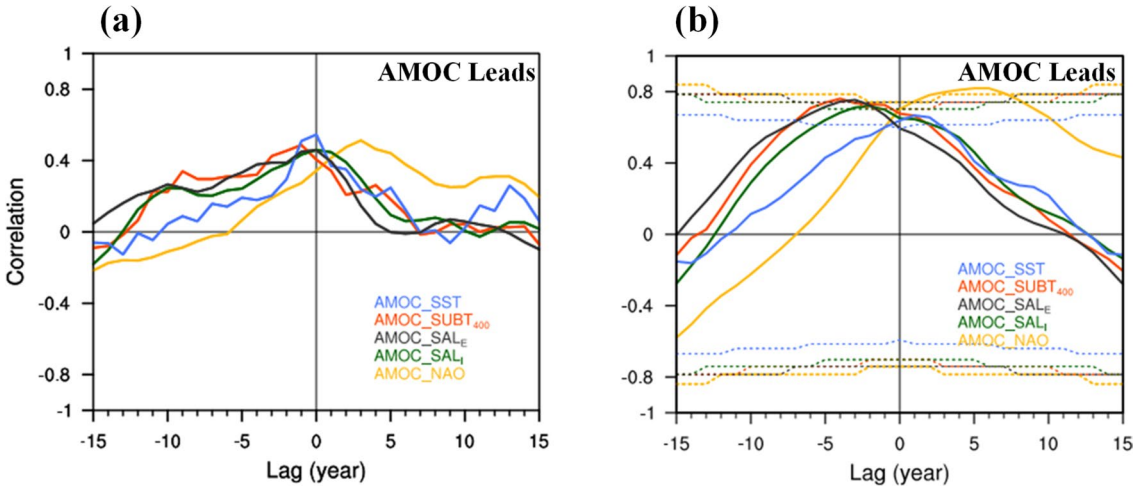

Fig. 7 **a** Lead-lag correlations between AMOC indicators and the SST Dipole during 1955–2015. The dipole index is defined by subtracting the South Atlantic SST from the North Atlantic SST. SST data is derived from the COBE dataset. The positive lag means the AMOC indices lead the dipole index. **b** As in **a**, but the SST data were processed by 11-year running mean and the long-term linear trend was removed. The dotted lines denote the 95% confidence levels for the correlations using the effective number of degrees of freedom

Dipole, consistent with previous modeling studies. And, the strong correlation between them is not determined by a single AMOC indicator but those using atmospheric and oceanographic variables. The discrepancies between atmospheric AMOC indicator and oceanic AMOC indicators is the time lag. It is because the AMOC_NAO index is based on the atmospheric forcing induced by the NAO which leads the AMOC by several years, while the subsurface temperature and ocean salinity need time to respond to the ocean heat transport induced by the AMOC. The simultaneous correlation between SST and SST Dipole also supports our explanations because the SST can directly respond to the surface ocean heat fluxes without any time delay.

Previous studies have suggested that the SST Dipole could influence the precipitation in NH tropics (Sun et al. 2013) and we've found the strong correlation between the AMOC and the SST Dipole. Thus, we can further use the SST Dipole to explain the physical mechanisms about the associations between the AMOC indicators and the mean precipitation in NH. When the NAO is positive, the anomalous atmospheric signal is stored in the ocean by imposing persistent forcing on the ocean circulation to implement the AMOC. There's a time lag between positive NAO and strengthened AMOC due to the large ocean dynamical inertia. AMOC plays an important role in transporting heat between two hemispheres, which leads to warming over the North Atlantic and cooling in the South Atlantic. Such a pattern is referred to as the SST Dipole. It further leads to the increase in SST gradients over the NH and in turn changes the atmospheric circulation (Hadley Cell), which is favorable for the anomalous low-level southerlies associated with the northward cross-equatorial winds. As a result, more water vapor is transported from the Southern Hemisphere to the Northern Hemisphere through the anomalous southerlies, moistening the atmosphere over Sahel and NH tropics. Correlations between SST and the observed precipitation in the Sahel (Fig. 8a) and NH (Fig. 8b) exhibit clear dipole patterns with strong positive correlations locate over the North Atlantic and negative correlations distribute over the South Atlantic. As shown in Fig. 8, the correlation patterns are highly consistent with that of the SST Dipole. To validate our results, we repeat the above analysis using multiple observational datasets (precipitation data are from CRU and GPCC; SST data are from HadISST and NOAA ERSST). The results are shown in Figs. S7–S9, and they all show consistent SST Dipole patterns, indicating that the close linkage between the SST Dipole and the precipitation in Sahel and NH is independent of the data selection.

The above mechanism has been proved in the modeling study (Sun et al. 2013) and it's physically reasonable to explain the relationship between SST Dipole and precipitation in the NH. However, the connection of precipitation to AMOC varies with regions. For example, the rainfall over the Sahel, northeastern Siberia and central North America exhibit prominent responses to the AMOC (Figs. 3 and 5). Therefore, it is of importance to explain the physical mechanisms of how the AMOC can influence the precipitation in these particular regions. As mentioned above, the SST dipole index is closely related to the AMOC indicators (Fig. 7), thus the AMOC may exert influences on the atmospheric circulation through the SST Dipole. As shown in Figs. 9a and 10a, the SST warming over the North Atlantic basin associated with the positive phase of SST dipole significantly modulates the large-scale atmospheric circulation,

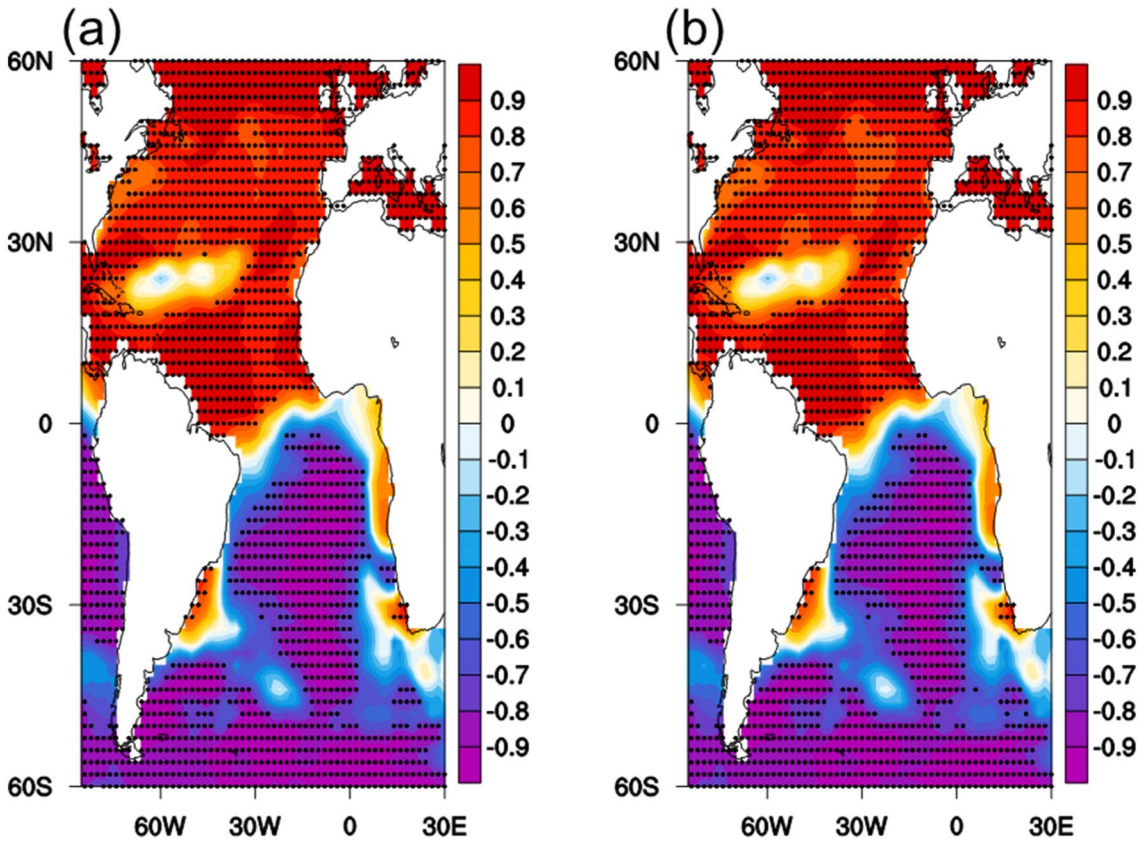

Fig. 8 **a** Correlations between annual mean precipitation in the Sahel and Atlantic SST from 1955 to 2015 at decadal timescales. **b** As in **a**, but for the Northern Hemisphere mean precipitation. The dotted areas denote correlations significantly above the 95% confidence level using the effective number of degrees of freedom

manifested by basin-wide low-pressure anomalies and the associated cyclonic flow over the North Atlantic and the adjacent regions (e.g., North Africa, North America and western Europe). More specifically, Sahel is governed by the anomalous southwest winds, exhibiting strong moisture convergence accompanied by the onshore moisture fluxes (Figs. 9a and 10a). Higher low-level moisture content and pronounced low pressure anomalies over the Sahel region are responsible for the significant increase in precipitation there. Previous studies have also suggested that the AMOC-induced SST changes in the Atlantic tend to influence the meridional movement of the Inter-tropical convergence zone (ITCZ), and the northward shift of ITCZ intensifies the ascending motion over the Sahel and is favorable for more precipitation (Knight et al. 2006; Zhang and Delworth 2006).

Meanwhile, the low-pressure anomalies and cyclonic flow over the North Atlantic induced by the North Atlantic warming lead to anomalous northerly winds over central North America (Fig. 9a). Corresponding to the northerly wind anomalies, strong moisture divergence could be found in over central North America, as shown in Fig. 10c. The anomalous northerly winds and associated divergence of moisture flux result in the decrease in moisture and drying over central North America (Fig. 10c). Our findings are consistent with the previous study (Sutton and Hodson 2005) that has provided observational and modeling evidence that North Atlantic warming is responsible for the atmospheric circulation changes and the associated rainfall variations over the United States.

Figure 9b shows the regressions of upper-level geopotential height and winds on the SST dipole index. The previous study (Sun et al. 2015c) provided both observational and modeling evidence to propose a Rossby wave train mechanism to explain the linkage between the Atlantic SST and the Siberian precipitation. Consistent with the previous study, the upper-level atmospheric circulation in response to the North Atlantic warming exhibits a clear wave train pattern across the Eurasian continent, and the upper-level flow is dominated by anomalous southerly winds over the eastern Siberia region. Corresponding to the upper-level flow, the low-level flow is characterized by southerly wind anomalies over the eastern Siberia which results in the anomalous moisture convergence as is shown

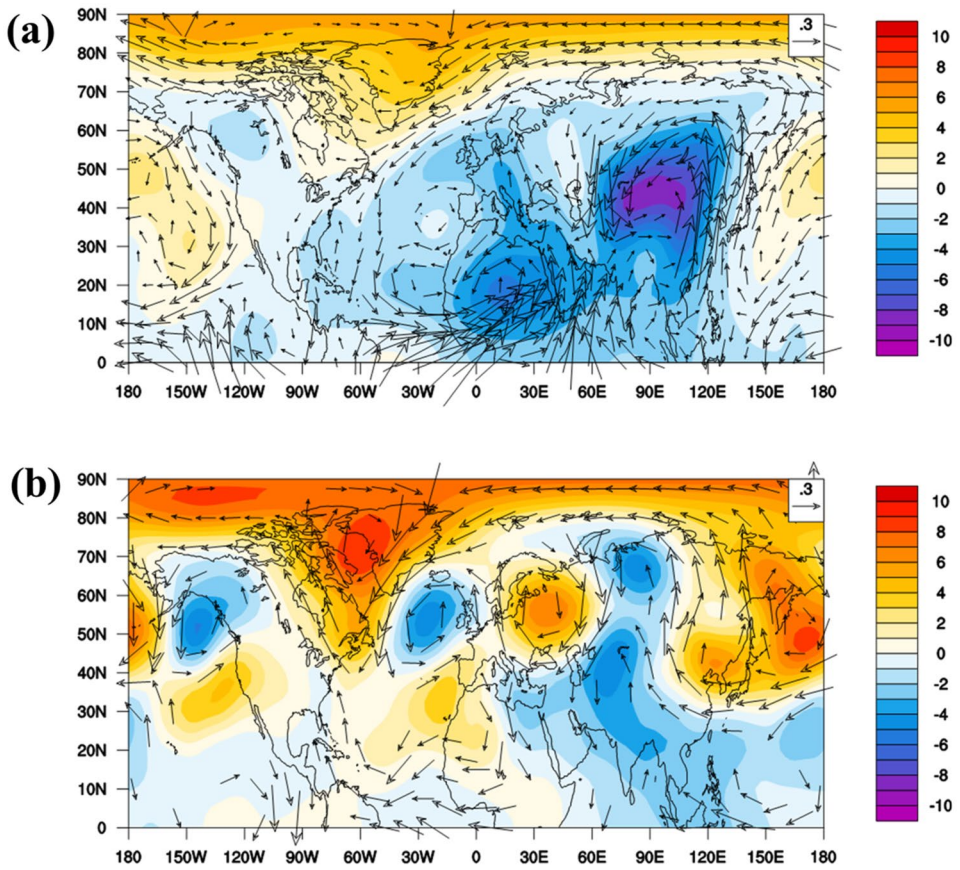

Fig. 9 **a** Regressions of 850 hPa geopotential height (shading, units: m) and winds (vectors, units: m/s) on the normalized SST dipole index at decadal time scales for the period 1955–2015. The SST dipole index is defined by subtracting the South Atlantic SST from the North Atlantic SST. SST data is derived from the COBE dataset. Only wind vector regressions that are significant at the 90% confidence level are shown. **b** As in **a**, but for 200 hPa geopotential height (shading, units: m) and winds (vectors, units: m/s). Atmospheric data are derived from the NCEP reanalysis

in Fig. 10b. The anomalous southerlies and associated convergence of moisture flux lead to a strong increase in the water vapor content over Siberia in response to the remote North Atlantic forcing. Meanwhile, the southerly convergent flow over the eastern Siberia is accompanied by low pressure anomalies, favorable for anomalous ascending motions in this region. Therefore, the local atmospheric circulation changes over the eastern Siberia is linked to the Atlantic SST variations through the Rossby wave train, and these atmospheric circulation changes are responsible for the increase in the precipitation.

3.4 Multidecadal prediction of NH precipitation

Based on the analysis of the associations of AMOC indicators with NH precipitation, the AMOC_NAO index exhibits its great potential to make predictions in NH precipitation. It is concluded from (1) the correlation between AMOC_NAO index and precipitation is very prominent; (2) the AMOC_NAO index leads the precipitation by 8 years. Thus, we establish a linear model using the AMOC_NAO index as a predictor to predict the multidecadal precipitation change in NH. The model is shown as follow:

$$\text{Precipitation}\,(t) = \text{aAMOC\_NAO}\,(t-8) + \text{b}t + \text{c}$$

where t is time in years. Coefficients a, b and c in the model are determined by regression analysis based on the historical data. In doing so, the root mean square error of the consequence from the observation and model is minimized. A similar model was constructed in a previous study to predict the East Asian surface air temperature based on the NAO (Xie et al. 2019). The training period of the prediction model is 1955–2017 for the precipitation data, and we use the AMOC_NAO during 1947–2009 for the training of the prediction model (Fig. 11). The AMOC_NAO during 2010–2017 is used to predict future changes in the precipitation. The formation of the AMOC_NAO indicator suggests the Atlantic Ocean integrates the NAO atmospheric variability and responds by causing changes in the AMOC, and the AMOC_NAO represents the accumulated effect of NAO atmospheric forcing on the ocean circulation. The low-frequency variation in the AMOC is implicitly considered in AMOC_NAO due to the integration and additional filtering of AMOC_NAO is not necessarily required. Here, we use the AMOC_NAO with no additional filtering as the predictor of the precipitation, and this ensures the continuity of the time series from the hindcast and prediction results. Model

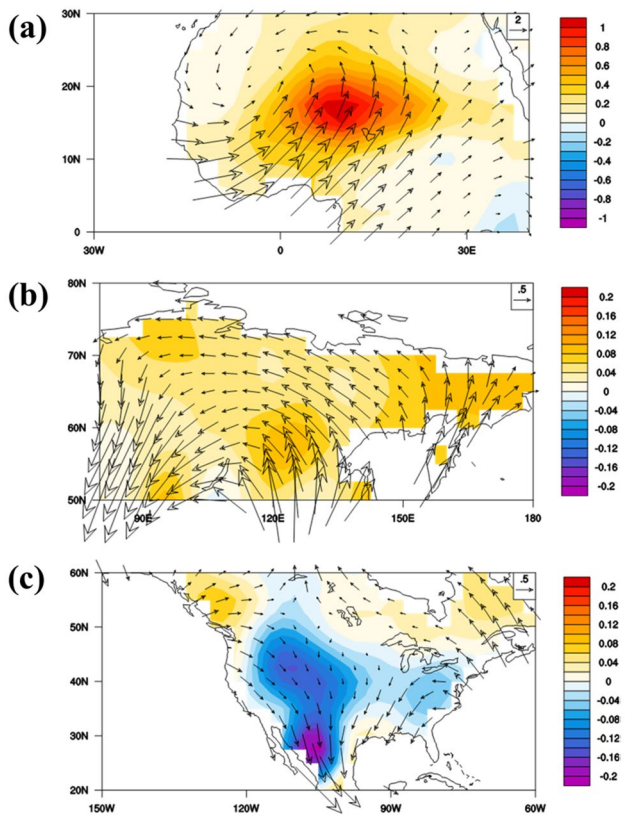

Fig. 10 Regressions of low-level (700–925 hPa average) moisture flux (vectors, units: kg m^{-1} s^{-1}, vertically integrated) and specific humidity (shading, units: g kg^{-1}) in North Africa on the normalized SST dipole index at decadal time scales for the period 1955–2015. **b** As in **a**, but for the moisture flux and specific humidity in eastern Siberia. **c** As in **a**, for the moisture flux and specific humidity in North America. Atmospheric data are derived from the NCEP reanalysis

performance is then examined, comparing to the historical observation.

Since the connection of precipitation to the AMOC_NAO index varies with regions, we examined the model performance from 1955 to 2017 in NH, NH tropics and Sahel, respectively. The decadal precipitation variations are well captured by the model, and most of the observed values fall in the uncertainty range. In Fig. 11a, the modeled time series of the NH precipitation fluctuates around the observation. It successfully reproduces the decreasing trend from 1955 to 1985 and the increasing trend after 1985. The model slightly overestimates the amplitude of the multidecadal variation but it's still consistent with the observation and the biases between them are within 1 mm/month. In NH tropics and Sahel, the modeled time series are also in good agreement with the observation. Overall, the model is capable of reproducing the trends in the observed precipitation and the inflection points are also in good agreement with the observation. Biases can be found around the years when the precipitation reaches extrema. Despite those small biases exist, the modeled series are still representative of the observed historical precipitation in all three regions. More importantly, the modeled time series in Sahel and NH are highly consistent with the observation in recent decades and that would reduce bias for future prediction.

Then, we use the model to predict future precipitation based on historical data. Since the model uses AMOC_NAO as a predictor which leads the precipitation by 8 years thus we can predict the precipitation in NH, NH tropics and Sahel during the period from 2018 to 2025. The predicted patterns in all three regions are highly consistent and they all share a rapidly decreasing trend in the following few years and then rise again. The changes in precipitation in the next 8 years are within 3 mm/month.

4 Conclusion and discussions

Precipitation is an essential factor that profoundly influences the industrial and agricultural productions and impacts on global economic growth. The multidecadal variability in precipitation has received considerable attention in recent years and has been proved to be associated with ocean dynamics by previous modeling studies. Thus, we further investigate the relationship between NH precipitation and the AMOC based on observational data instead.

In this study, we find that the multidecadal variability in NH precipitation is robust and significant from 1955 to 2015. The mean precipitation in Sahel and NH tropics also shares a similar variation with a decreasing trend from 1955 to 1985 and an increasing trend in recent three decades. We employ five AMOC indicators based on the observed oceanic and atmospheric variables to represent the strength of AMOC and examine their spatial correlations with the observed NH precipitation. It suggests that precipitation in the Sahel, NH tropics and northeastern Siberia is simultaneously correlated with the oceanic AMOC indicators, while the AMOC_NAO index strongly correlates with the precipitation when it leads by 8 years. The correlation between NH precipitation and SST exhibits a strong dipole pattern resembles the Interhemispheric SST Dipole that also correlates with the AMOC_NAO index at a time lag of 8 years. It further explains the mechanism between AMOC and NH precipitation, that is, NAO imposes persistent forcing on the ocean and further leads to AMOC. Northward ocean heat transport associated with AMOC induces the North Atlantic warming and South Atlantic cooling called the SST Dipole. The SST Dipole increases the SST gradients over the NH and induces anomalous cross-equatorial southerlies that transport the water vapor, contributing to the increased precipitation in NH tropics and Sahel region.

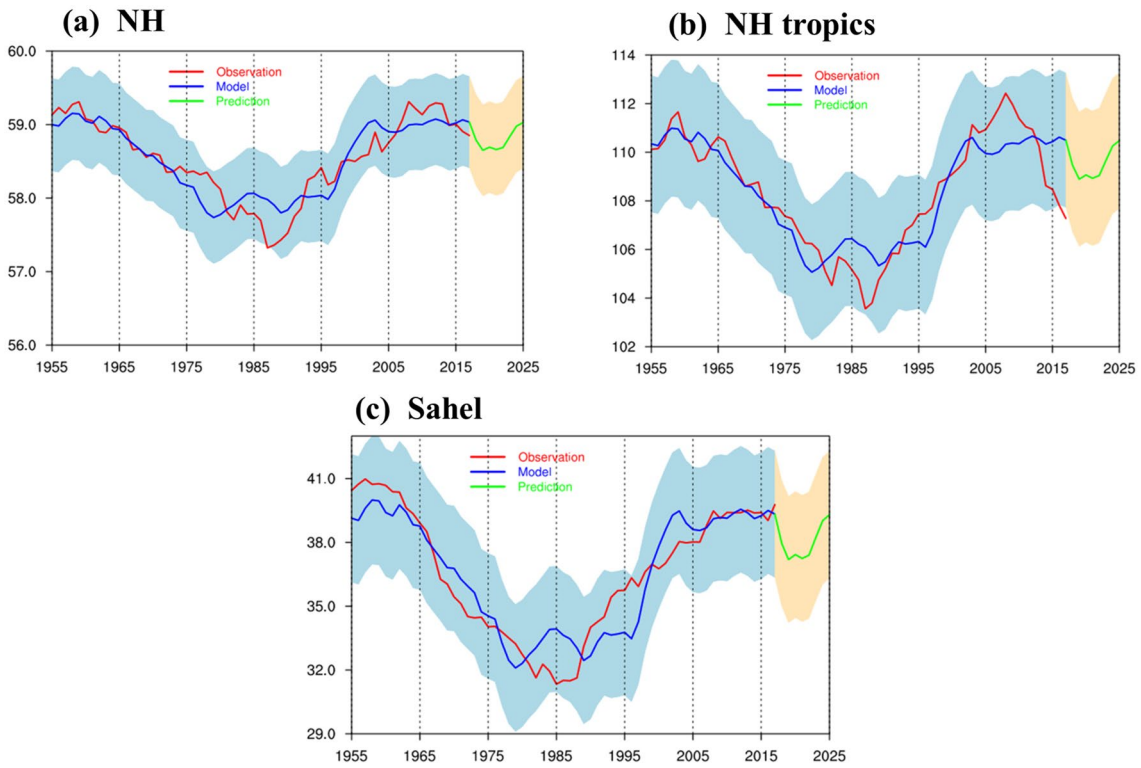

Fig. 11 Observed, modeled, and predicted decadal precipitation (mm/month). Observed annual precipitation (red) for 1955–2017, modeled annual precipitation (blue) for 1955–2017, and predicted annual precipitation (green) for 2018–2025 over Northern Hemisphere (**a**), Northern Hemisphere tropics (**b**) and Sahel (**c**). The shaded areas show the 2-sigma uncertainty range of the model predicted values

Since the AMOC_NAO index significantly correlates with the NH precipitation when it leads by 8 years, the AMOC_NAO index exhibits unique potentials as a predictor for NH precipitation. Thus, we construct a linear model based on this index and predict the precipitation changes in the following 8 years. The modeled series are in good agreement with the historical precipitation data. The precipitation in Sahel, NH tropics and NH will experience a rapidly decreasing trend in the next few years and then will rise again till 2025.

Our work evaluates the responses of the observed precipitation to the five AMOC indicators based on oceanic and atmospheric variables. It provides valid observational evidence that the NH precipitation strongly correlates with the AMOC. We also find a way to explain the mechanism of how the AMOC influences the NH precipitation. More importantly, AMOC_NAO leads the precipitation by 8 years and is used here to make future predictions. Questions remain as a significant correlation between northeastern Siberia precipitation and the AMOC that needs further investigation. Moreover, paleoclimate studies would extend our knowledge over a longer time scale to further examine the validity of our findings. Coupled model simulations should also put into practice to answer why the NAO-based indicator can better explain the NH precipitation over other indices.

Acknowledgements We would like to thank the anonymous reviewers for their constructive comments that helped improve our manuscript. This work was jointly supported by National Key Research and Development Program of China (2020YFA0608401) and the National Natural Science Foundation of China (41975082, 41775038 and 41790474).

References

Barlow M, Nigam S, Berbery EH (2001) ENSO, Pacific decadal variability, and U.S. summertime precipitation, drought, and stream flow. J Clim 14:2105–2128

Becker A, Finger P, Meyer-Christoffer A, Rudolf B, Schamm K, Schneider U, Ziese M (2013) A description of the global land-surface precipitation data products of the Global Precipitation Climatology Centre with sample applications including centennial (trend) analysis from 1901-present. Earth Syst Sci Data 5:71–99. https://doi.org/10.5194/essd-5-71-2013

Boer GJ (2011) Decadal potential predictability of twenty-first century climate. Clim Dyn 36:1119–1133

Boer GJ et al (2016) The Decadal Climate Prediction Project (DCPP) contribution to CMIP6. Geosci Model Dev 9:3751–3777

Bretherton CS, Widmann M, Dymnikov VP, Wallace JM, Bladé I (1999) The effective number of spatial degrees of freedom of a time-varying field. J Clim 12:1990–2009

Broecker WS (1998) Paleocean circulation during the last deglaciation: a bipolar seesaw? Paleoceanography 13:119–121

Buckley MW, Marshall J (2016) Observations, inferences, and mechanisms of the Atlantic Meridional Overturning Circulation: a review. Rev Geophys 54:5–63

Burckel P et al (2015) Atlantic Ocean circulation changes preceded millennial tropical South America rainfall events during the last glacial. Geophys Res Lett 42:411–418
Caesar L, Rahmstorf S, Robinson A, Feulner G, Saba VS (2018) Observed fingerprint of a weakening Atlantic Ocean overturning circulation. Nature 556:191–196
Chen X, Tung K (2018) Global surface warming enhanced by weak Atlantic overturning circulation. Nature 559:387–391
Delworth TL, Mann ME (2000) Observed and simulated multidecadal variability in the Northern Hemisphere. Clim Dyn 16:661–676
Doblasreyes FJ et al (2013) Initialized near-term regional climate change prediction. Nat Commun 4:1715
Dong B, Dai AG (2015) The influence of the interdecadal Pacific oscillation on temperature and precipitation over the globe. Clim Dyn 45:2667–2681. https://doi.org/10.1007/s00382-015-2500-x
Fred K et al (2016) The teleconnection of the tropical Atlantic to Indo-Pacific sea surface temperatures on inter-annual to centennial time scales: a review of recent findings. Atmosphere 7:29
Garciagarcia D, Ummenhofer CC (2015) Multidecadal variability of the continental precipitation annual amplitude driven by AMO and ENSO. Geophys Res Lett 42:526–535
Gulev S, Latif M (2015) Ocean science: the origins of a climate oscillation. Nature 521:428–430
Hu Q, Feng S (2012) AMO- and ENSO-driven summertime circulation and precipitation variations in North America. J Clim 25:6477–6495
Hurrell JW (1995) Decadal trends in the North Atlantic oscillation: regional temperatures and precipitation. Science 269:676–679
Keenlyside N, Latif M, Jungclaus JH, Kornblueh L, Roeckner E (2008) Advancing decadal-scale climate prediction in the North Atlantic sector. Nature 453:84–88
Knight JR, Folland CK, Scaife AA (2006) Climate impacts of the Atlantic multidecadal oscillation. Geophys Res Lett 33:L17706
Latif M et al (2004) Reconstructing, monitoring, and predicting multidecadal-scale changes in the North Atlantic thermohaline circulation with sea surface temperature. J Clim 17:1605–1614
Lee SK, Wang C (2010) Delayed advective oscillation of the Atlantic thermohaline circulation. J Clim 23:1254–1261
Li J, Sun C, Jin F (2013) NAO implicated as a predictor of Northern Hemisphere mean temperature multidecadal variability. Geophys Res Lett 40:5497–5502
Li X, Xie S-P, Gille ST, Yoo C (2016) Atlantic-induced pan-tropical climate change over the past three decades. Nat Clim Change 6:275–279. https://doi.org/10.1038/nclimate2840
Mccarthy GD, Haigh ID, Hirschi JJM, Grist JP, Smeed DA (2015) Ocean impact on decadal Atlantic climate variability revealed by sea-level observations. Nature 521:508–510
Mecking J, Keenlyside N, Greatbatch RJ (2014) Stochastically-forced multidecadal variability in the North Atlantic: a model study. Clim Dyn 43:271–288
Meehl GA et al (2009) Decadal prediction: can it be skillful? Bull Am Meteorol Soc 90:1467–1485
Oreilly CH, Huber M, Woollings T, Zanna L (2016) The signature of low-frequency oceanic forcing in the Atlantic Multidecadal Oscillation. Geophys Res Lett 43:2810–2818
Parsons LA, Yin J, Overpeck JT, Stouffer RJ, Malyshev S (2014) Influence of the Atlantic Meridional Overturning Circulation on the monsoon rainfall and carbon balance of the American tropics. Geophys Res Lett 41:146–151
Pyper BJ, Peterman RM (1998) Comparison of methods to account for autocorrelation in correlation analyses of fish data. Can J Fish Aquat Sci 55:2127–2140
Rahmstorf S, Box JE, Feulner G, Mann ME, Robinson A, Rutherford S, Schaffernicht E (2015) Exceptional twentieth-century slowdown in Atlantic Ocean overturning circulation. Nat Clim Change 5:475–480
Rayner NA (2003) Global analyses of sea surface temperature, sea ice, and night marine air temperature since the late nineteenth century. J Geophys Res 108(D14):4407
Srokosz MA et al (2012) Past, present, and future changes in the Atlantic meridional overturning circulation. Bull Am Meteorol Soc 93:1663–1676
Sun C, Li J, Jin F, Ding R (2013) Sea surface temperature inter-hemispheric dipole and its relation to tropical precipitation. Environ Res Lett 8:044006
Sun C, Li J, Feng J, Xie F (2015a) A decadal-scale teleconnection between the North Atlantic Oscillation and subtropical eastern Australian rainfall. J Clim 28:1074–1092
Sun C, Li J, Jin F (2015b) A delayed oscillator model for the quasi-periodic multidecadal variability of the NAO. Clim Dyn 45:2083–2099
Sun C, Li J, Zhao S (2015c) Remote influence of Atlantic multidecadal variability on Siberian warm season precipitation. Sci Rep 5:16853
Sun C, Li J, Ding R, Jin Z (2017) Cold season Africa-Asia multidecadal teleconnection pattern and its relation to the Atlantic multidecadal variability. Clim Dyn 48:3903–3918
Sun C, Li J, Li X, Xue J, Ding R, Xie F, Li Y (2018) Oceanic forcing of the interhemispheric SST dipole associated with the Atlantic Multidecadal Oscillation. Environ Res Lett 13:074026
Sun C et al (2020) Atlantic Meridional Overturning Circulation reconstructions and instrumentally observed multidecadal climate variability: a comparison of indicators. Int J Climatol 40:1–16
Sutton RT, Hodson DLR (2005) Atlantic Ocean forcing of North American and European summer climate. Science 309:115–118
Teegavarapu RSV, Goly A, Obeysekera J (2013) Influences of Atlantic multidecadal oscillation phases on spatial and temporal variability of regional precipitation extremes. J Hydrol 495:74–93
Trenberth KE, Caron JM (2001) Estimates of meridional atmosphere and ocean heat transports. J Clim 14:3433–3443
Valdespineda R, Canon J, Valdes JB (2018) Multi-decadal 40- to 60-year cycles of precipitation variability in Chile (South America) and their relationship to the AMO and PDO signals. J Hydrol 556:1153–1170
Vellinga M, Wood RA (2002) Global climatic impacts of a collapse of the Atlantic thermohaline circulation. Clim Change 54:251–267
Veres MC, Hu Q (2013) AMO-forced regional processes affecting summertime precipitation variations in the central United States. J Clim 26:276–290
Wang C, Dong S, Evan AT, Foltz GR, Lee S (2012) Multidecadal covariability of North Atlantic sea surface temperature, African dust, Sahel rainfall, and Atlantic hurricanes. J Clim 25:5404–5415
Xie T, Li J, Sun C, Ding R, Wang K, Zhao C, Feng J (2019) NAO implicated as a predictor of the surface air temperature multidecadal variability over East Asia. Clim Dyn 53:895–905
Yan X, Zhang R, Knutson TR (2017) The role of Atlantic overturning circulation in the recent decline of Atlantic major hurricane frequency. Nat Commun 8:1695
Zhang R (2008) Coherent surface-subsurface fingerprint of the Atlantic meridional overturning circulation. Geophys Res Lett 35:L20705
Zhang R, Delworth TL (2006) Impact of Atlantic multidecadal oscillations on India/Sahel rainfall and Atlantic hurricanes. Geophys Res Lett 33:123–154